ELSEVIER

Journal of Power Sources 113 (2003) 209–227

JOURNAL OF POWER SOURCES

www.elsevier.com/locate/jpowsour

New modified AGM separator and its influence on the performance of VRLA batteries

D. Pavlov[a,*], V. Naidenov[a], S. Ruevski[a], V. Mircheva[b], M. Cherneva[a]

[a]*Central Laboratory of Electrochemical Power Sources, Bulgarian Academy of Sciences, 1113 Sofia, Bulgaria*
[b]*Institute of Polymers, Bulgarian Academy of Sciences, 1113 Sofia, Bulgaria*

Abstract

A new modified AGM (MAGM) separator for VRLA batteries and the respective technology for its production have been developed. The new product is obtained by processing absorbent glass mat (AGM) separator with polymer emulsion, which is adsorbed onto the surface of the glass fibres and concentrates at the sites of contact between the fibres. Thus, a continuous porous network of interconnected glass fibres is formed. The two surfaces of the AGM sheet are treated with polymer emulsion of different concentration in view of the different processes that take place at the positive and the negative plates, respectively. As a result of the above treatment the surface properties of the AGM are modified to balance hydrophobic/hydrophilic properties. The MAGM separator has improved tensile strength as compared to untreated AGM, a slightly reduced H_2SO_4 absorption and wicking rate, and increased chemical and thermal stability. It does not disperse in H_2SO_4 solution as does AGM. The influence of the MAGM separator on the processes in the valve-regulated lead-acid cell has been investigated. An experimental method has been elaborated and used to establish the existence of horizontal electrolyte stratification between the plates. This stratification is a result of the different processes that occur at the two types of plates as well as of the resistance that the ion flows of H_2SO_4 and H_2O have to overcome when passing through the separator. In VRLA batteries, their movement is impeded by the AGM separator, which reduces the available capacity of the battery. The effect of the MAGM separator on the concentration of H_2SO_4 at the two separator interfaces during charge, discharge, open circuit (OC) and on cycling is investigated. MAGM influences the processes in the cells in such a way that the differences in H_2SO_4 concentration between the two types of plates are eliminated. These effects of the MAGM separator result in an increase of the available capacity of the battery on cycling and float service, which leads to a substantial increase in VRLA battery life. Moreover, MAGM improves the efficiency of the oxygen cycle in the cells and thus the water loss is reduced. Besides, MAGM separators reduce the differences in cell voltage when numerous cells are connected in long strings.

Keywords: Lead-acid battery; Modified AGM; VRLAB; Electrolyte stratification; Charge and discharge of LA batteries

1. Introduction

It has been established that during battery operation, the concentration of H_2SO_4 changes along the height of the lead-acid cell, increasing in its lower parts [1]. This phenomenon was called stratification. The influence of current density on electrolyte stratification and on the available capacity of the lead-acid cell was studied in papers [2,3].

The question arises whether there is stratification of the H_2SO_4 electrolyte in the horizontal direction, i.e. between the positive and the negative plates, during battery operation? On charge and discharge, the concentration of H_2SO_4 ($C_{H_2SO_4}$) in the positive and the negative plates changes, but at different rates, as a result of which a difference in $C_{H_2SO_4}$ is created between the two plates. H_2SO_4 and water are the only mobile active materials, which can move between the positive and the negative plates. In VRLA cells the amount of electrolyte is considerably reduced and the movement of H_2SO_4 and H_2O is impeded by the absorbent glass mat (AGM) separator. Thus, a concentration polarization may occur in the cell, which shortens the discharge time and increases the cell voltage during charge. The first aim of the present work was to provide experimental evidence of phenomenon horizontal electrolyte stratification.

When studying this phenomenon, the parameter time should be taken into account. What time is needed for the $C_{H_2SO_4}$ in/at the two types of plate to become equal on open circuit (OC)? What parameters influence the levelling of these concentrations when the battery is left on open circuit? To answer these questions, it is necessary to introduce into the battery analysis the parameter *H_2SO_4 distribution in the*

* Corresponding author. Tel.: +359-2-718651; fax: +359-2-731552.
E-mail address: dpavlov@mbox.cit.bg (D. Pavlov).

0378-7753/02/$ – see front matter
PII: S0378-7753(02)00516-5

lead-acid cell with time. The latter depends on the mobility of H_2SO_4 ions (e.g. H^+, SO_4^{2-}) and H_2O within the cell volume. The second aim of the present investigation was to determine the $C_{H_2SO_4}$ in the interface layers of the separator for two different time periods: immediately after charge or discharge and after a 24-h stay of the battery on open circuit. The differences in H_2SO_4 concentration between the positive and the negative plates were determined by measuring the $C_{H_2SO_4}$ *in the interface layers of the separator with the positive plate (Sep/PPlate) and with the negative plate (Sep/NPlate), respectively.* A special experimental method was designed for this purpose.

Another question arises in this context: Whether we can influence the transport of H_2SO_4 between the positive and the negative plates and thus minimize the effect of the H_2SO_4 distribution with time on VRLA battery performance? This was the main goal of the present study. The AGM separator was modified with the help of polymer emulsions of balanced hydrophobic and hydrophilic properties, which allowed the surface properties of the glass fibres to be changed. This would result in:

(a) changes in the mobility of the H^+ and SO_4^{2-} ions and of H_2O through the separator, and
(b) changes in the transport rate of O_2 flows between the two types of plates, when an oxygen cycle is active.

For the purpose of the investigation, we developed a modified AGM (MAGM) separator by processing commercial AGM with polymer emulsion [4,5]. The present paper will discuss first the structure and properties of the MAGM separator, then the influence of AGM and MAGM on the transfer of H_2SO_4 through the separator during charge, discharge, cycling and on open circuit (tests were performed using cells), and the third part of the paper will focus on the effect of the new MAGM separator on battery performance.

2. Experimental

2.1. AGM and MAGM separators

The following method was developed for the purpose of measuring the H_2SO_4 concentration at the two separator surfaces and thus proving experimentally the existence of horizontal stratification. Two types of absorbent glass mat separators produced by Hollingsworth & Vose (USA) were used, one with a thickness of 2.5 mm (440 g/m^2) and the other one with a thickness of 0.2 mm (30 g/m^2). The thinner AGM sheet served for measuring the $C_{H_2SO_4}$ at the Sep/Plate interfaces. For this purpose, one sheet of the thinner (0.2 mm) separator was attached to each side of the thicker (2.5 mm) separator sheet. Thus, three-layered separators with an overall thickness of 2.9 mm were obtained.

The modified AGM separator was produced by processing each surface of the thick AGM separator sheet with a polymeric emulsion of a definite composition and concentration. One side of the thick separator was treated with concentrated emulsion and the other side with diluted one. This was done in an attempt to achieve an appropriate balance between the hydrophilic and hydrophobic properties of the separator, which would facilitate the transport of H_2SO_4 ions and of water and oxygen through the separator. Then the MAGM was thermally treated employing an appropriate program.

The two thin separator sheets were processed using the same technology, but one of them was processed with concentrated polymer emulsion and the other one with diluted one. Each of the thin sheets was attached to the respective side of the thicker MAGM sheet, thus yielding a three-layered MAGM separator. Both AGM and MAGM sheets were sized 140 mm × 153 mm and were then introduced into the cells.

The above multi-sheet separator was used only when the H_2SO_4 concentration at the Sep/NPlate and Sep/PPlate interfaces had to be determined. For determining the influence of MAGM or AGM on battery performance characteristics only one thick separator sheet was introduced into the cells.

2.2. Lead-acid cells for measuring the horizontal stratification

The cells contained one negative and two positive plates with a three-layered separator on both sides of the negative plate (Fig. 1). The degree of saturation of the separators and of the plates with H_2SO_4 was 96%. The capacity of the cells was 11 Ah or 10 Ah and it was limited by the capacity of the negative plate. This active block was placed in a plexiglass cell with thick walls, one of which was mobile to allow the compression of the cell to be varied. Investigations were carried out with 8 or 25% compression of the separators. Cells of the following three types were tested:

(a) reference cells with AGM separators (AGM cells). These were assembled using three-layered AGM separator not treated with polymer emulsion;
(b) cells with MAGM separators whose surface treated with low-concentration polymer emulsion faced the negative plate (denoted as MAGM-L cells);
(c) cells with MAGM separators whose surface treated with high-concentration polymer emulsion faced the negative plate (denoted as MAGM-H cells).

The cells were virtually divided in three horizontal zones: upper (up), middle (mid) and bottom (bot), and three vertical zones: positive lug side (+lug), central (c) and negative lug side (−lug) (Fig. 1). Thus, nine virtual mini-cells were obtained. The H_2SO_4 concentration at the Sep/NPlate and Sep/PPlate interfaces was measured in the above nine mini-cells using a refractometer (Fig. 1).

The $C_{H_2SO_4}$ results of some of the tests are presented as mean arithmetic values for the three vertical mini-cells and

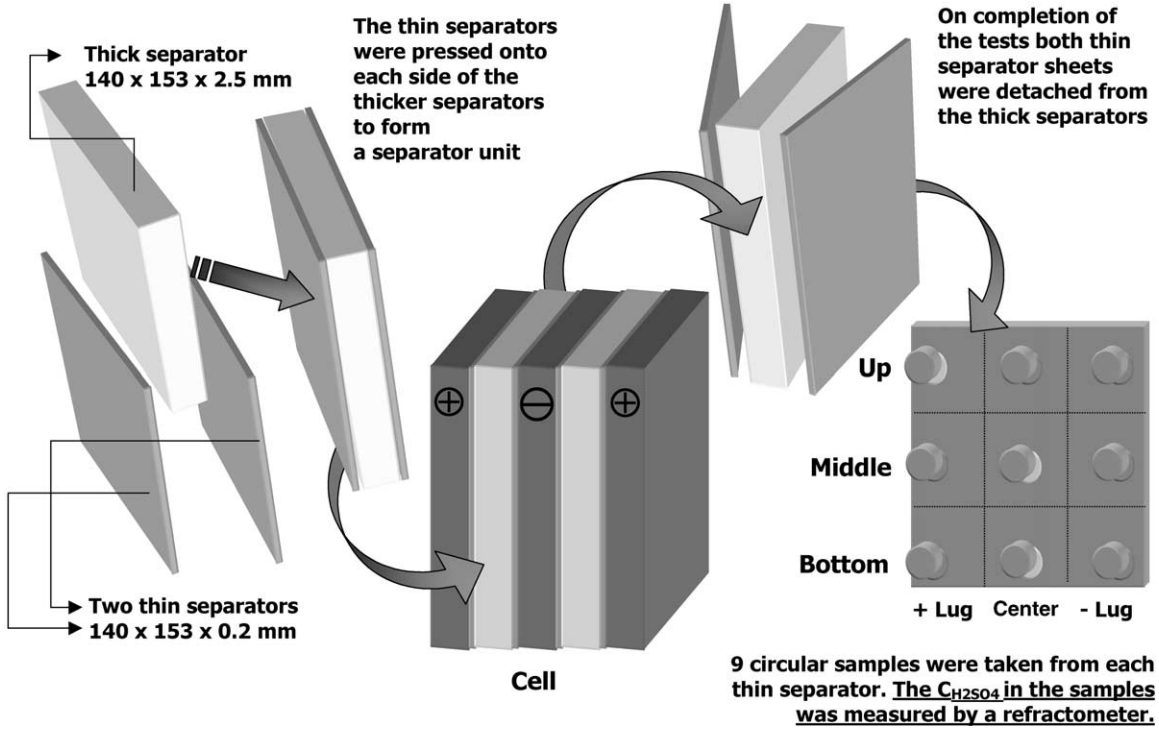

Fig. 1. Method for measuring the H_2SO_4 concentration at the separator interfaces with the positive and negative plates.

in other tests the values measured for each virtual mini-cell are given separately, which provides the instant distribution of the $C_{H_2SO_4}$ in all nine virtual mini-cells.

2.3. Charge–discharge algorithm

The cells were set to charge–discharge cycling using a Bitrode LCN testing equipment. Charging was conducted with $I_1 = 5$ A until 2.50 V was reached and this voltage ($U_2 = 2.50$ V) was maintained until charge factor 115%. The discharge current was $I = 2.20$ A corresponding to 5 h discharge down to a cut-off-voltage of 1.70 V or $I = 0.22$ A corresponding to 50 h discharge. All tests were performed at a constant temperature of 25 °C.

2.4. H_2SO_4 concentration at the separator/positive plate (Sep/PPlate) and separator/negative plate (Sep/NPlate) interfaces

Five charge–discharge cycles were carried out for cell conditioning. Then the measurements started on charge or discharge. On completion of the tests, the cells were taken apart and the two three-layered separators were taken out (Fig. 1). Both thinner separator sheets (one facing the positive plate and the other one facing the negative one) were detached from the thick separators and circular samples were cut from each of the sheets. Samples were taken from each of the nine virtual mini-cells (Fig. 1). The H_2SO_4 concentration in these samples was measured with a refractometer.

2.5. Wicking test procedure

The H_2SO_4 absorption properties of MAGM were determined. Strips of AGM or MAGM with dimensions 170 mm × 20 mm were dipped vertically to a depth of 10 mm into 1.28 s.g. H_2SO_4 solution (with an addition of methylorange to tint the solution). The following determinations were made:

(a) Acid absorption—the amount of electrolyte absorbed by the sample for 20 min, calculated in g H_2SO_4/g separator.
(b) Wicking rate—assessed from the height to which the solution creeps up the AGM or MAGM strip under the action of the capillary forces for a given time period. The height was measured every minute for a period of 15 min.

The wicking test was performed using a non-compressed (free) or compressed separator strip.

3. Experimental results and discussion

3.1. Structure, mechanical and physico-chemical properties of AGM and MAGM separators

3.1.1. Structure of AGM and MAGM

The structure of the AGM and MAGM separators was determined through scanning electron microscopy (SEM). Fig. 2 shows SEM micrographs of the structure of untreated

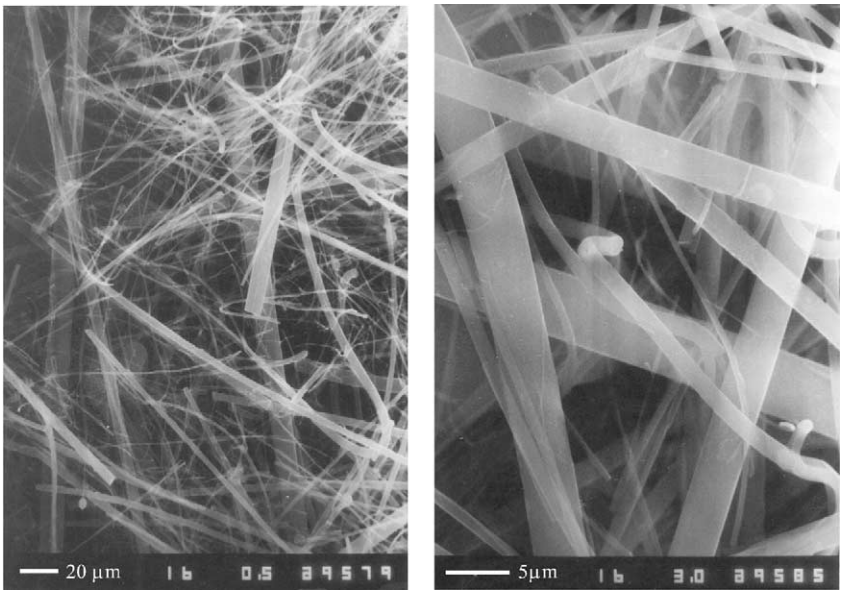

Fig. 2. SEM micrographs of the structure of AGM separator at two magnifications.

AGM. This material features a combination of loose fibres, with smaller and larger diameters, which are scattered chaotically and are not interconnected.

Fig. 3 shows SEM micrographs of the structure of the MAGM separator. The modifying emulsion concentrates at the sites of contact between the fibres. The polymer emulsion interconnects the AGM fibres into a continuous network. Thus, the separator is converted into a highly porous "plate" with definite surface properties. Hence, the first advantage of MAGM is that the interrupted structure of AGM is converted into a non-interrupted structure in MAGM with specific surface properties determined by the composition of the modifying polymer emulsion and the process of MAGM treatment.

3.1.2. Tensile strength

Sample strips with dimensions 28 mm × 152 mm were set to tensile tests. Table 1 summarizes the results obtained for AGM and MAGM. In order to be able to make accurate comparison between the tensile strength of AGM and MAGM the former was dipped in the same amount of water as that of the polymer emulsion used for treatment of the MAGM (30 ml per sheet). After that the AGM sheet was dried until a constant weight was achieved and then cut into

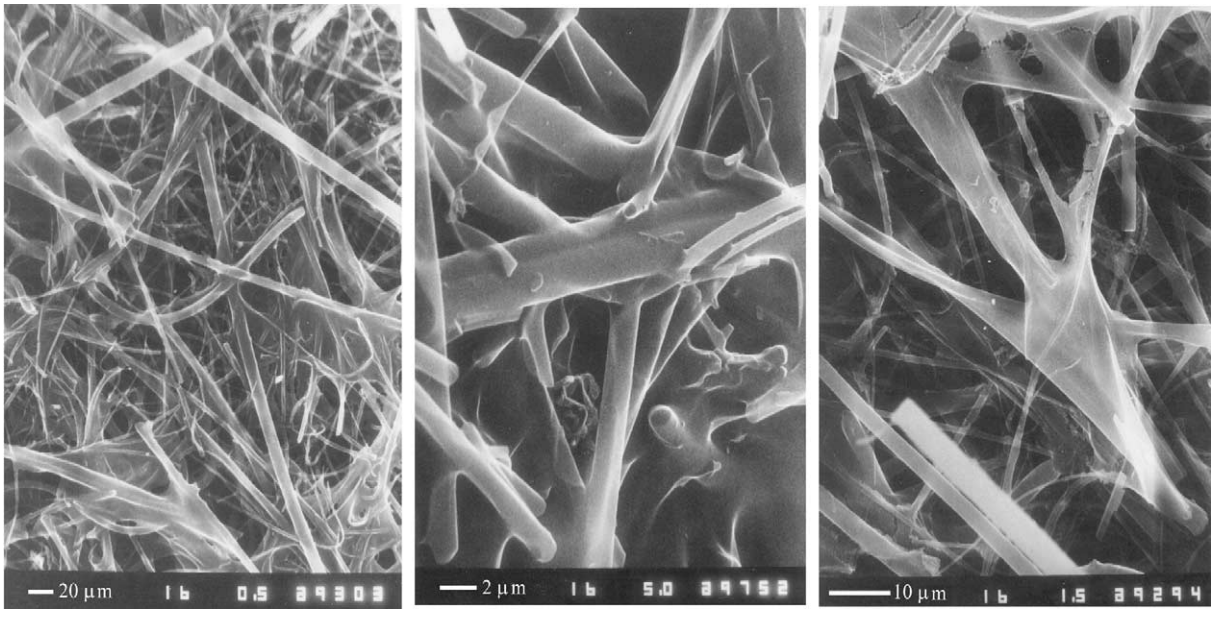

Fig. 3. SEM micrographs of the structure of MAGM separator at various magnifications.

Table 1
Tensile strength of AGM and MAGM

S. no.	Type of AGM (MAGM)	Tensile strength (kg)
1	AGM commercial, dry	1.46
2	AGM unilaterally treated with water (30 ml per sheet) and then dried	0.83
3	AGM bilaterally treated with water (50 ml per sheet) and then dried	0.77
4	MAGM	1.38

strips of the above size which were used for the tensile tests. The measured tensile strength values for the thus moistened and dried AGM separator are given in Table 1 together with tensile strength data for commercial AGM.

When the AGM separator is moistened its tensile strength decreases by 53–57%.

Though treated with the same amount of liquid emulsion, the MAGM has considerably higher tensile strength than the water treated AGM. The tensile strength of the MAGM decreases by about 5% as compared to untreated commercial AGM, but is higher by ca. 66% than that of the water-treated-and-then-dried AGM. MAGM does not disperse in H_2SO_4 solution or in H_2O as does AGM.

3.1.3. Acid absorption test results

It has been established that AGM absorbs 8.25 g H_2SO_4/g AGM against 7.2 g H_2SO_4/g MAGM. Hence, modification of AGM with polymer emulsion reduces the acid absorption by about 13%.

Compressed AGM and MAGM samples were also set to acid absorption tests employing the BCI test procedure. Table 2 gives the acid absorption data obtained for AGM and MAGM.

Table 2
Acid absorption data for 2.5 mm thick samples of AGM and MAGM

Separator type	g H_2SO_4/g separator	Saturation (%)
AGM	6.87	94.1
MAGM	6.58	94.7

Saturation time, 2 h. Compression, 22%.

At 22% compression the two types of separators have almost equal acid absorption and saturation.

3.1.4. Wicking rate

Fig. 4a illustrates the wicking test results obtained for non-compressed strips of AGM and MAGM separators. H_2SO_4 with s.g. 1.28 was used. It can be seen that the capillary forces have the strongest action in AGM and the sulphuric acid creeps rapidly up the sample strips. A slightly weaker effect have the capillary forces in MAGM.

Fig. 4b presents the wicking test results for compressed (22%) separator strips (2.5 mm thick) of AGM and MAGM. H_2SO_4 with s.g. 1.30 was used. The H_2SO_4 wicking rate measured for the MAGM separator is slightly lower than that for AGM, but is still sufficiently high and will not affect the technological time taken for filling the cells with H_2SO_4 solution.

3.1.5. Chemical and thermal stability of AGM and MAGM separators

The chemical and thermal stability of the AGM and MAGM separators were assessed from the concentration of Na^+ and K^+ ions in samples of equal surface area immersed in 200 ml of H_2SO_4 with s.g. 1.28 after soaking stay in the solution at 60 °C for 7 days. Samples of the solution were taken and the concentration of Na^+ and K^+ ions in them was determined. The results obtained are given in Table 3.

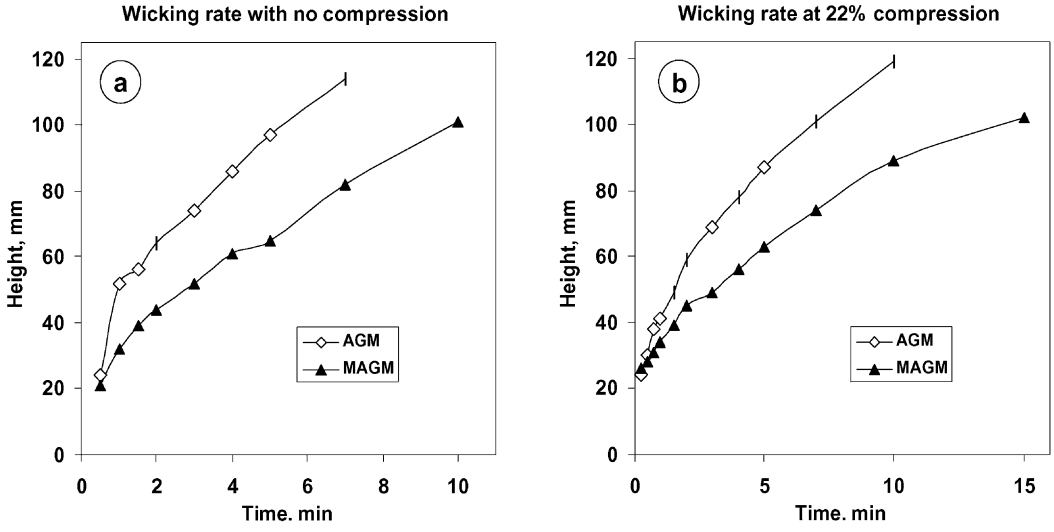

Fig. 4. Wicking rate of H_2SO_4 solution in AGM and MAGM separators with no compression and with 22% compression applied.

Table 3
Solubility of Na^+ and K^+ ions from AGM and MAGM samples in H_2SO_4 solution s.g. 1.28

Type of separator	Na^+ (g/l)	K^+ (g/l)
AGM	0.74	0.020
MAGM	0.64	0.015

It can be generally concluded that modification of the AGM separator improves its chemical and thermal stability by about 13–25%.

3.2. Horizontal electrolyte stratification: tests of AGM and MAGM cells

The reactions that proceed in the positive and negative plates during charge and overcharge of VRLAB with closed oxygen cycle are presented schematically in Fig. 5. The figure shows the directions of the flows of H^+ ions, H_2O and O_2 through the AGM separator.

As is evident from the figure, water is consumed at the separator/positive plate interface and hence the H_2SO_4 concentration will increase. At the separator/negative plate interface water is formed and $C_{H_2SO_4}$ will decrease. Thus, different H_2SO_4 concentrations are formed at the two separator interfaces as a result of the reactions involved in the oxygen cycle.

Investigations were carried out with cells with AGM, MAGM-L (low polymeric concentration on the side facing the negative plate) and MAGM-H (high polymeric concentration on the side facing the negative plate). The compression of all three cells was 8%. After charging up to a charge factor $F_{ch} = 115\%$, the H_2SO_4 concentration at the two interfaces was measured. The measurements were performed immediately after charge and after 24 h stay on open circuit. Fig. 6 presents the results obtained for three horizontal separator zones of the three types of cells. The average concentration for each zone was calculated as the mean arithmetic value of the three measurements for the three vertical zones.

The following conclusions can be drawn from the figure:

- *AGM cells*: The H_2SO_4 concentration at the Sep/NPlate interface is lower than that at the Sep/PPlate one. This difference is 0.010 g/cm^3 for the upper zone of the cell and 0.029 g/cm^3 for the bottom zone, respectively. These experimental results are in support of the conclusion drawn from Fig. 5. After 24 h rest on open circuit, the horizontal difference in H_2SO_4 concentration decreases but does not disappear. These data confirm the existence of horizontal electrolyte stratification.
- *MAGM-L cells*: In this cell, too, horizontal differences in H_2SO_4 concentration are observed immediately after charging of the cell, but after 24 h stay on open circuit, only a small difference remains in the bottom zone of the cell.
- *MAGM-H cells*: There is no difference between the H_2SO_4 concentrations at the two interfaces of the MAGM-H separator. This indicates that the MAGM-H separator facilitates the transport of H_2SO_4 and H_2O between the two types of plates, which prevents the formation of horizontal electrolyte stratification.

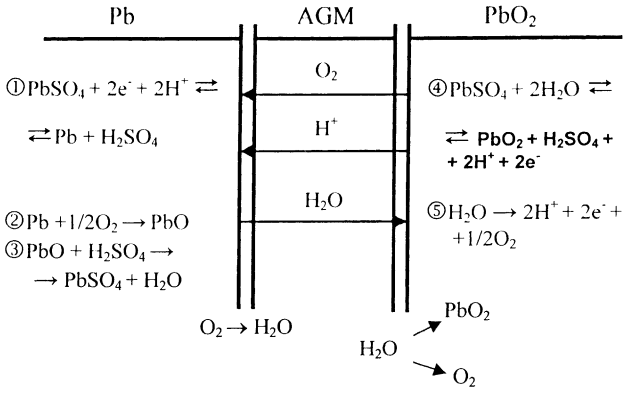

Fig. 5. Reactions that proceed in the lead-acid cell during charge and when an oxygen cycle is operative.

Based on the data in Fig. 6, the distribution of H_2SO_4 in the three horizontal zones with time can be represented schematically for the three types of cells. Fig. 7 shows the $C_{H_2SO_4}$ distribution for the AGM cell after charge (a.ch.) and after 24 h stay on open circuit (24 h). During charge the H_2SO_4 concentration increases both in the positive and in the negative plates. However, the diffusion flows between the two types of plates are strongly impeded by the AGM separator. This creates horizontal electrolyte stratification in the cell. During the 24 h rest on open circuit, flows of H_2SO_4 get into the separator from both types of plates and the H_2SO_4 concentration in the cell tends to equalize that in the plates. However, this cannot be fully accomplished in 24 h and the $C_{H_2SO_4}$ in the positive plates remains higher than that in the negative ones. Hence, AGM presents a barrier to the H_2SO_4 and H_2O ion flows and may thus limit the capacity of the cell.

Fig. 8 presents the distribution of H_2SO_4 concentration in the cell with MAGM-L separators immediately after charge and after 24 h rest on open circuit. The electrolyte concentration in the negative plates is kept higher than in the separators as a result of which the $C_{H_2SO_4}$ at the Sep/NPlate interface increases during the 24 h stay of the cell on open circuit. At the Sep/PPlate interface the H_2SO_4 concentration is higher in the separator than in the positive plate. This is probably due to the O_2 evolved at the positive plate. The polymer emulsion used to modify the AGM separator is more concentrated at its interface with the positive plate. This may impede the access of water formed at the negative plate by the reduction of oxygen. Thus, the

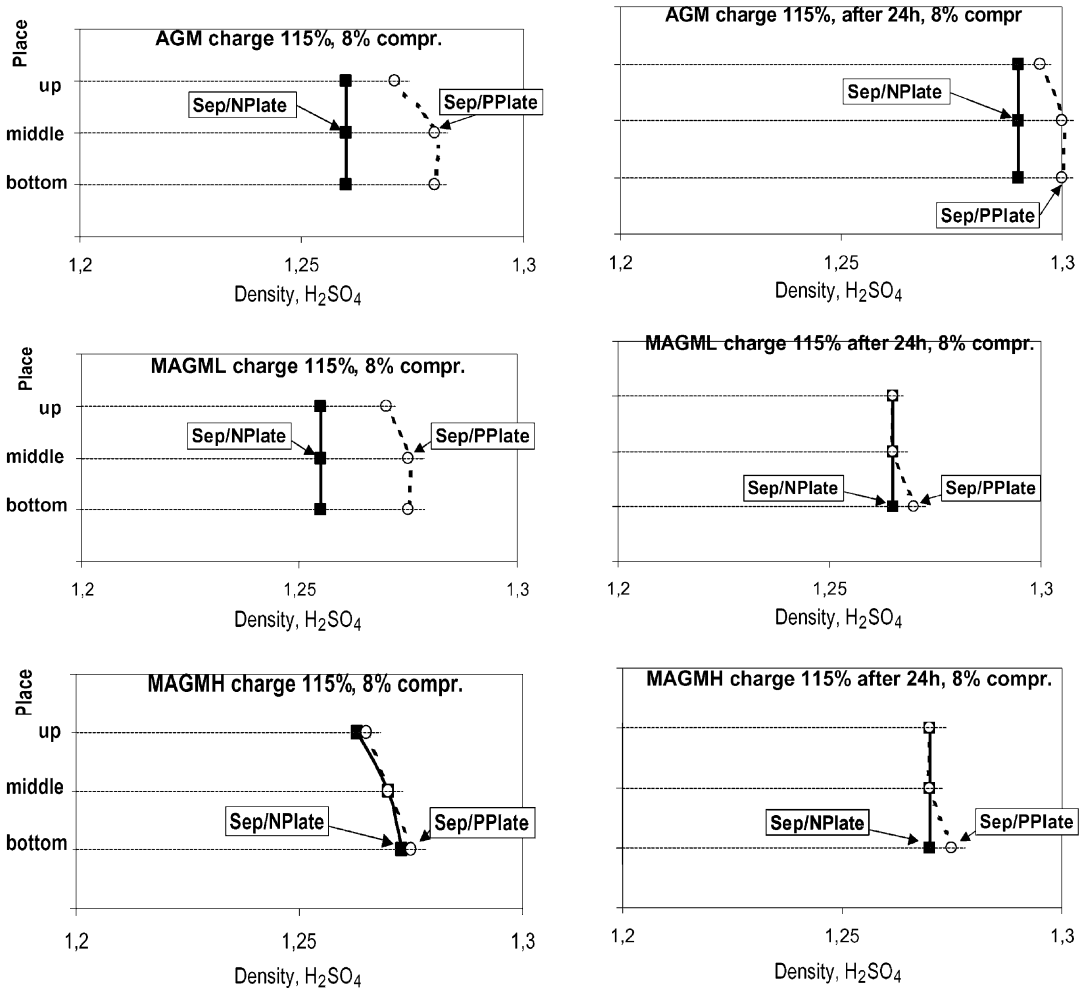

Fig. 6. H_2SO_4 concentration at the Sep/PPlate and Sep/NPlate interfaces measured in the three horizontal zones of cells with AGM, MAGM-L and MAGM-H separators immediately after charge and after 24 h stay on open circuit.

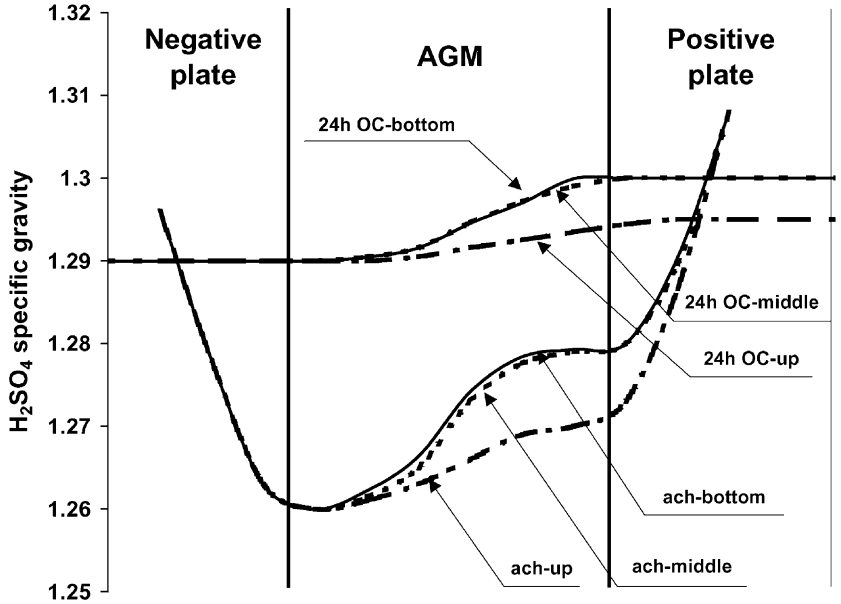

Fig. 7. H_2SO_4 concentration profile for the three horizontal zones of AGM cells immediately after charge and after 24 h stay on open circuit.

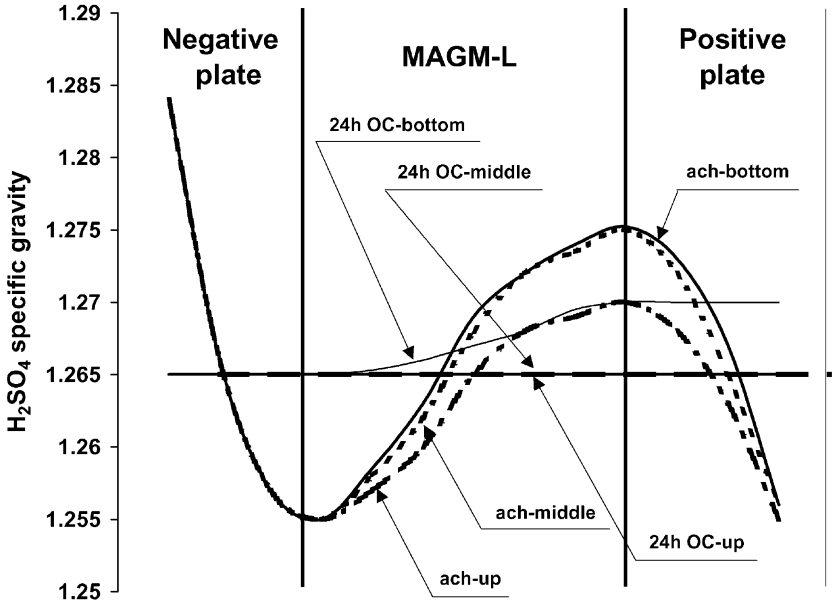

Fig. 8. H_2SO_4 concentration profile for the three horizontal zones of MAGM-L cells immediately after charge and after 24 h stay on open circuit.

surface properties of the separator fibres near the interface with the positive plate will cause the formation of a higher H_2SO_4 concentration there. During the stay on open circuit, the H_2SO_4 will try to distribute uniformly both in the positive plate and in the separator, and maybe a certain flow of H_2SO_4 will reach the negative plate after all in an attempt to level the H_2SO_4 concentration throughout the cell.

Fig. 9 shows the distribution of $C_{H_2SO_4}$ in the plates and in the separator of a MAGM-H cell. During charge and as a result of the oxygen cycle (charge factor, $F_{ch} = 115\%$), the H_2SO_4 concentration in the negative plate is slightly lower than that in the upper and lower zones of the positive plates. In their middle zones both types of plates have the same H_2SO_4 concentration. After rest on open circuit, the H_2SO_4 concentration is levelled in the upper and middle zones of the cell, whereas in the bottom zones it remains slightly higher at the Sep/PPlate interface. In this particular cell the separator surface treated with more concentrated polymer emulsion faces the negative plate. It could be expected that surface of the separator treated thus, will push away the water evolved at the negative plate towards the positive one and thus facilitate levelling of the H_2SO_4 concentration in the cell, which is actually observed. Thus, MAGM-H eliminates the horizontal stratification of electrolyte.

The data in Figs. 7–9 also indicate that the H_2SO_4 concentration in the AGM cell is higher than that in the two types of MAGM cells. All three cells were assembled with the same types of plate and, prior to formation, were filled with the same amount of H_2SO_4 with s.g. 1.25. The increase in H_2SO_4 concentration in the AGM cell is a result of water loss. For 30 cycles before the above measurement, this water loss is much greater for the AGM cell than for the MAGM ones.

3.3. H_2SO_4 concentration at the two separator interfaces during discharge of the LA cell

The following reactions proceed during discharge of a lead-acid battery:

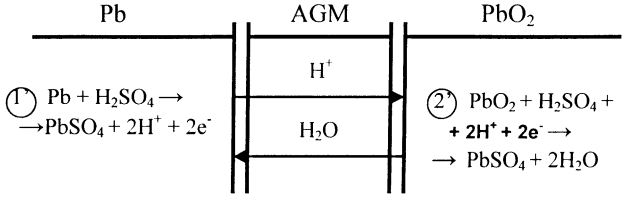

The H_2SO_4 amount in the solution filling the pores of the plates and of the two separator interfaces decreases. Moreover, water is formed on the positive plate which dilutes further the H_2SO_4 solution at the Sep/PPlate interface. The H_2SO_4 concentration was measured in all nine mini-cells of both separator interfaces at different DOD. The results obtained are presented in Fig. 10 for the cells with AGM separtors.

The following conclusions can be drawn from the figure:

(a) The three zones of the cells exhibit different states of discharge. The middle zone is discharged most deeply and the bottom part is the least discharged one.
(b) The H_2SO_4 solution at the Sep/PPlate interface is not always more diluted than that at the Sep/NPlate interface. It should be taken into account that the cell comprised one negative and two positive plates, and thus the effect of dilution of H_2SO_4 in the positive plates would be reduced as it is split between the two positive plates.
(c) The discharge process does not proceed at the same rate in the horizontal direction either. Most often the

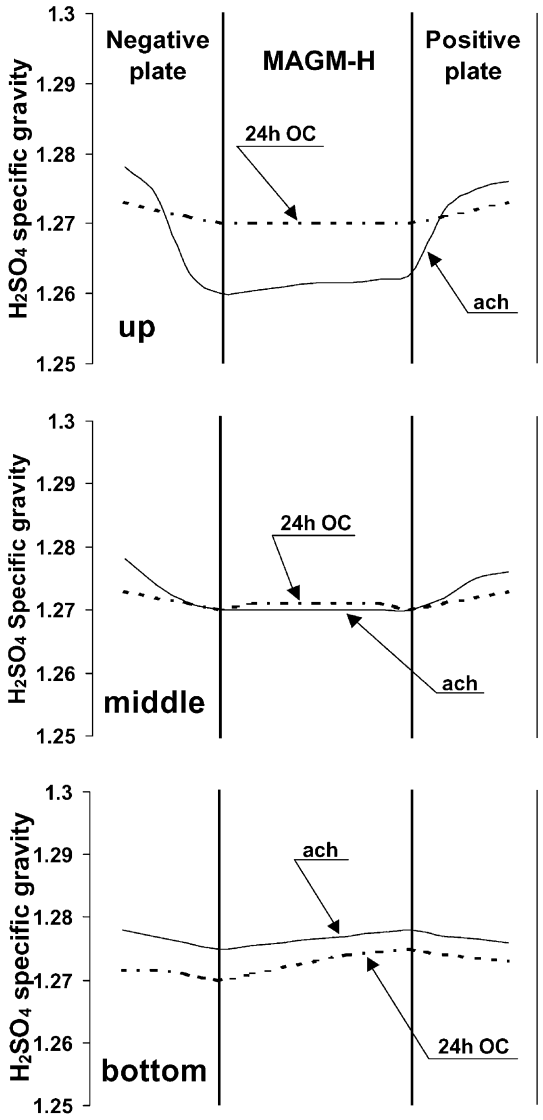

Fig. 9. H_2SO_4 concentration profile for the three horizontal zones of MAGM-H cells immediately after charge and after 24 h stay on open circuit.

deepest discharge is observed in the central zones of the plates. This is most probably related to the higher pH of the solution in the central virtual mini-cells.

Fig. 10 shows that the H_2SO_4 concentration at the Sep/PPlate interface is considerably higher than that at the Sep/NPlate one at DOD = 55 and 73%, which is in disagreement with reaction (2′). This indicates that at this DOD an electrochemical reaction proceeds at the positive plate in which H_2SO_4 does not take part. The product of this electrochemical reaction is not $PbSO_4$, but some kind of non-sulphate compound. In our previous investigations of the discharge reactions at the positive plate, we have established that besides $PbSO_4$ considerable amounts of orthorhomb-PbO are also formed [6]. The changes in total pore volume (V_t) and in solid phase density (d_V) during discharge of the positive plate have been followed [7]. It has been found that at 40% DOD the experimental V_t and d_v values are higher than the ones determined by the Faraday equation for reaction (2′) [7]. This finding was related to the formation of PbO and PbO_x ($x < 2$) if, however, the plates are left in H_2SO_4 for more than 16 h, the V_t and d_V values obtained are equal to the ones calculated by the Faraday equation for the $PbSO_4$ end product, i.e. PbO and PbO_x undergo sulphation [7]. The higher H_2SO_4 concentration measured at the Sep/PPlate interface during the second half of discharge (Fig. 10) is in good agreement with the results reported in [6,7] evidencing formation of PbO and PbO_x ($x < 2$) during positive plate discharge.

3.4. Influence of separator on the cycle life of the cells

Cells (10 Ah) were assembled with AGM, MAGM-L and MAGM-H separators and set to consequent cycling tests employing three different modes:

(a) discharge with $I_d = C_5/5$ A for 20–25 cycles, i.e. first cycling stage;
(b) discharge with $I_d = C_5/50$ A for 3–5 cycles, i.e. second stage;
(c) addition of water to the cells, i.e. the VRLA cells were transformed into flooded ones, and subjected to further cycling under mode (a) with $I_d = C_5/5$ A until the cell capacity fell below 7 Ah.

The H_2SO_4 concentration at both separator interfaces was measured during the first two cycling stages of discharged cells.

Fig. 11 shows the capacity curves obtained for the three types of cell. The cycle life of the cell with MAGM-H separator is about 45% longer than that of the AGM cell. The capacity of the MAGM-H cell is about or above the rated value (10 Ah) for almost 80% of its life span. The available capacity of the cells with AGM falls below the rated value (C_0) already within the first 10 cycles and remains about 80% of C_0 until the end of the first cycling stage. The cell with MAGM-L has available capacity equal to about 90% of the rated capacity values. It can be concluded then that the available capacity of the cells depends on the properties of the separator used.

Fig. 12 gives the time of charge until a charge factor of 115% is reached for the three types of cells. The charging time is shorter for the cells with MAGM-H and MAGM-L separators as compared to the AGM cell. This holds for both the first cycling stage (i.e. VRLAB) and the third stage when the cells are flooded with electrolyte. These results indicate that the MAGM separator improves the charge efficiency of the cell.

Fig. 13 presents the end-of-charge voltage versus number of cycles curves for the three types of cell. The cells with MAGM-H and MAGM-L separators have a bit lower charge voltage than that of the AGM cell. Both the shorter charging time and the lower charge voltage of MAGM cells indicate that the latter have lower internal resistance than the cell with AGM separator, which is obviously related to the properties of the separator used.

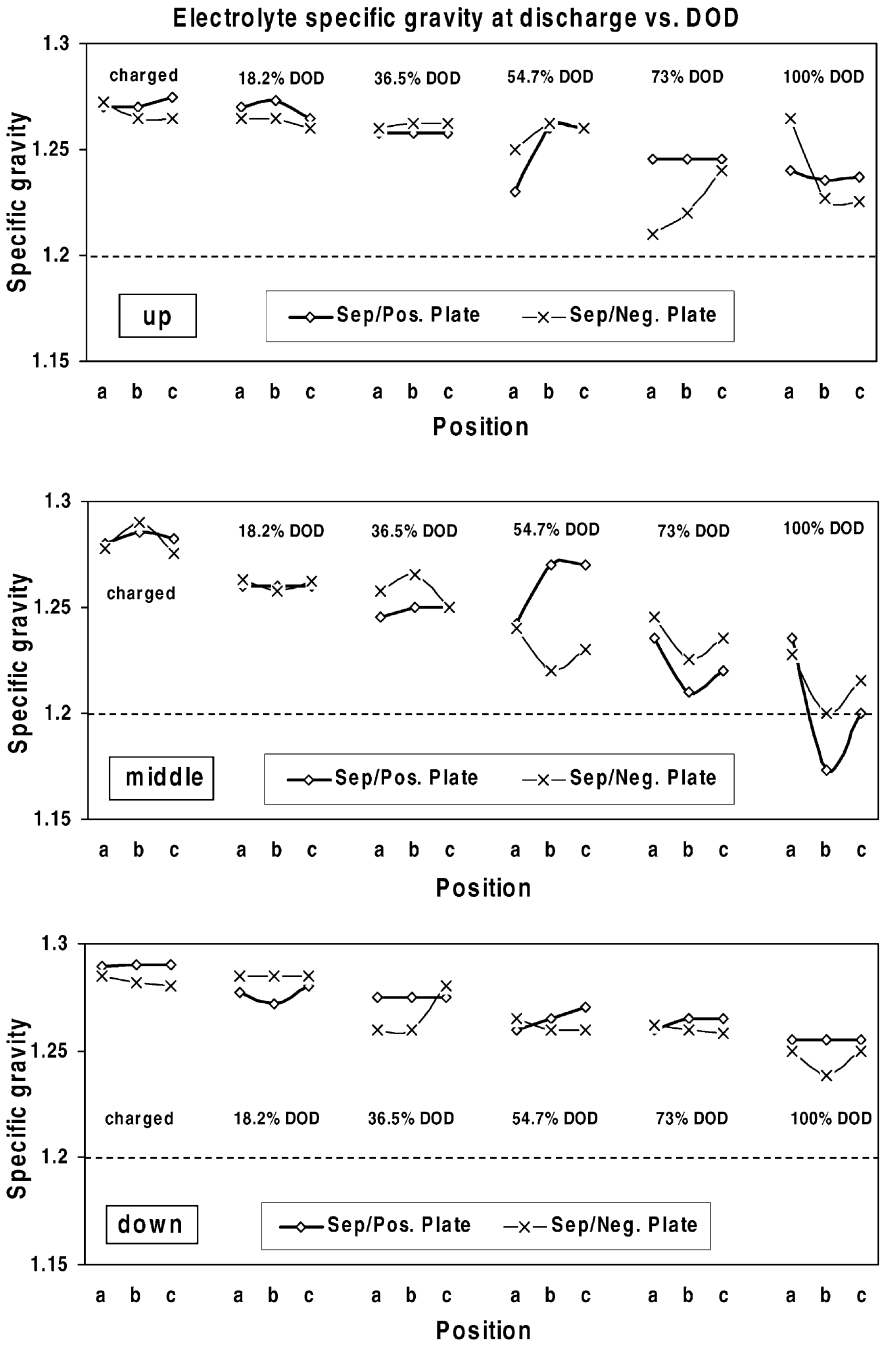

Fig. 10. H_2SO_4 concentration measured in the nine virtual mini-cells of the two separator interfaces of a AGM cell as depending on the DOD.

Fig. 14 shows the H_2SO_4 concentrations measured at both interfaces of the two separators of the cell held at open circuit for 24 h after 5 h discharge at the 20 h cycle. The mean arithmetic values of the twelve H_2SO_4 concentration measurements for each virtual mini-cell are also given in the figure.

It follows from the data in this figure that:

(a) Stratification of H_2SO_4 along the height of the cells is most pronounced in the cell with AGM separator and it is the smallest for the MAGM-H cell.

(b) Discharge of the cells is deepest in the cell with MAGM-H separator and most shallow in the AGM cell. This is in agreement with the results presented in Fig. 11.

Tables 4 and 5 summarize the mean arithmetic values of the H_2SO_4 concentrations measured at the three cell heights on cycling of the cells at 5 and 50-h rate of discharge, respectively. The concentrations were measured immediately after discharge and after 24 h stay of discharged cells on open circuit.

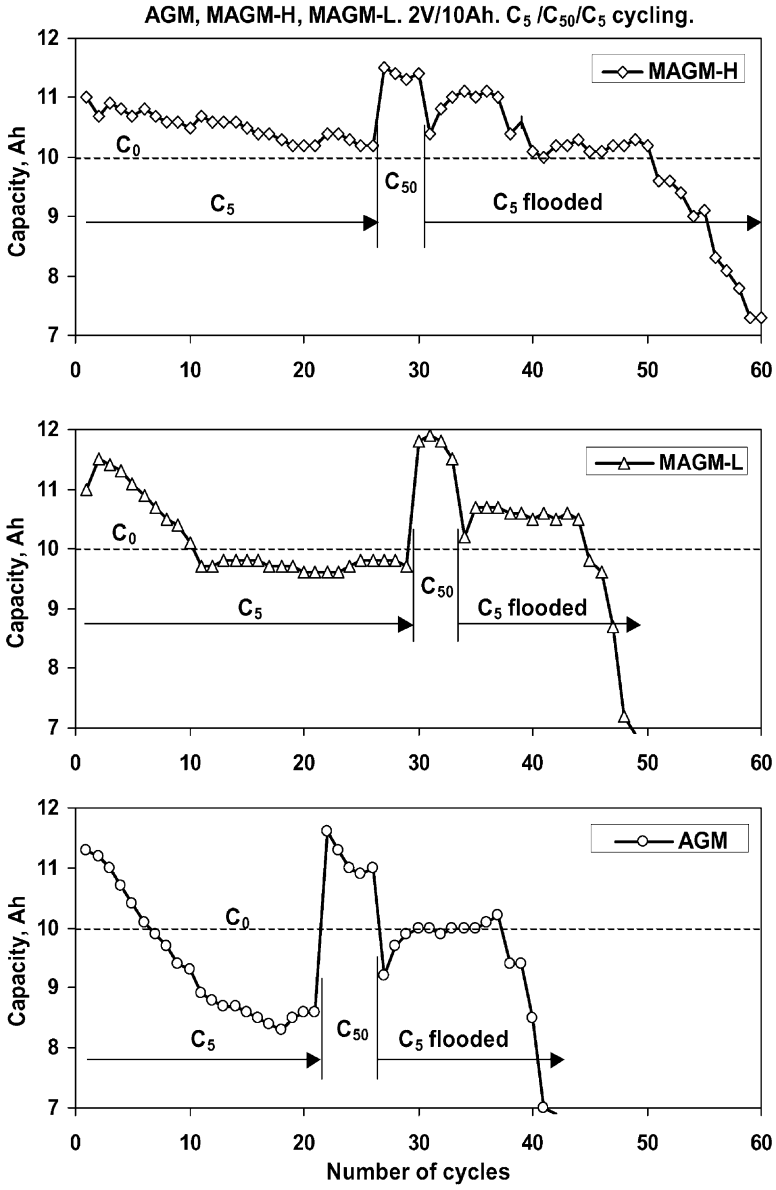

Fig. 11. Capacity vs. number of cycles dependencies for cells with AGM, MAGM-L and MAGM-H separators.

The data in Table 4 indicate that the average H_2SO_4 concentration in the cells compares as follows: $C_{H_2SO_4}$-(AGM) > $C_{H_2SO_4}$(MAGM-L) > $C_{H_2SO_4}$(MAGM-H), when the cells are cycled with $I_d = C_5/5$ A. Table 5 shows that on cycling with $I_d = C_5/50$ A, the average H_2SO_4 concentration in the cells in the discharged state is $C_{H_2SO_4}$(AGM) > $C_{H_2SO_4}$(MAGM-L) ≈ $C_{H_2SO_4}$(MAGM-H). Hence, the separator exerts an influence on the capacity of both AGM and

Table 4
Average H_2SO_4 concentration at Sep/PPlate and Sep/NPlate interfaces after cycling at 5 h rate of discharge

Position	AGM		MAGM-L		MAGM-H	
	Immediately after discharge	After 24 h OC	Immediately after discharge	After 24 h OC	Immediately after discharge	After 24 h OC
Up	1.250	1.233	1.209	1.220	1.205	1.205
Middle	1.240	1.235	1.219	1.230	1.207	1.209
Bottom	1.262	1.293	1.277	1.271	1.257	1.243
Cell average concentration	1.250	1.254	1.235	1.240	1.223	1.219

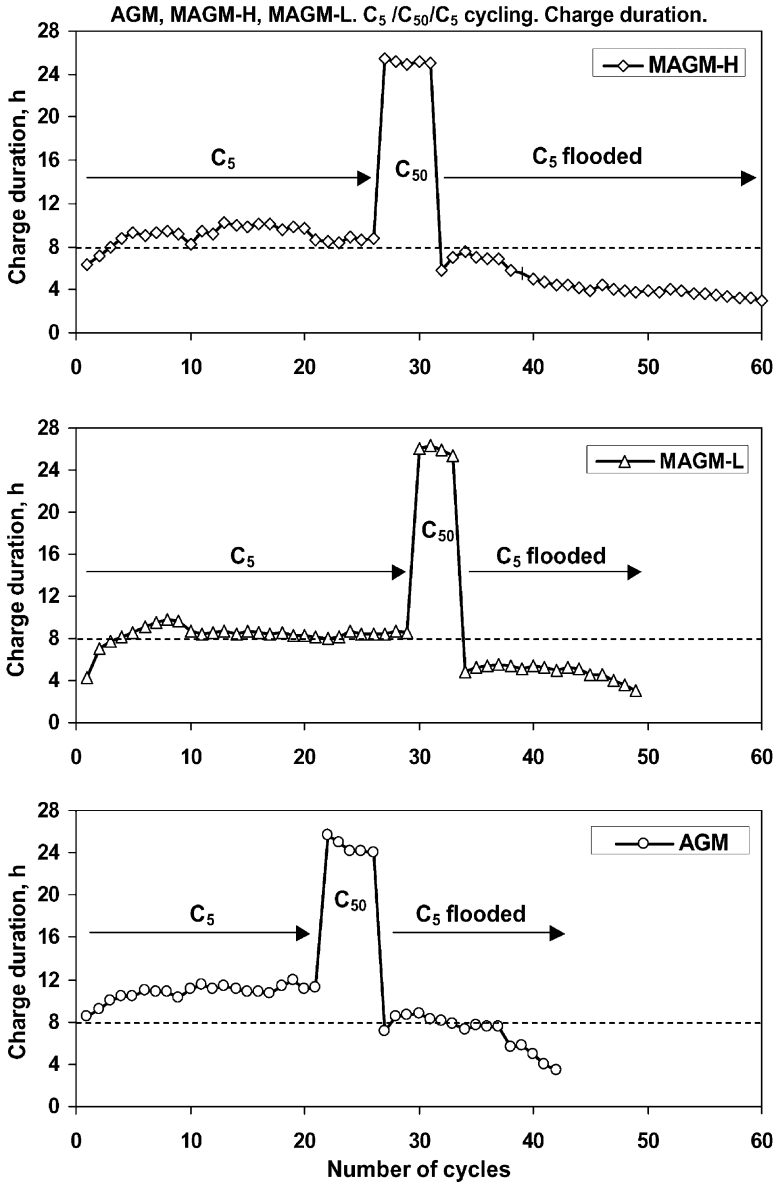

Fig. 12. Charge time (at $C_F = 115\%$) for the three types of cell cycled employing the three cycling modes.

MAGM cells. The role of the concentration of the modifying polymer emulsion on the properties of the two MAGM surfaces is less pronounced on cycling of the cells with a very weak current.

On comparing the data in Figs. 11 and 14 and in Table 4, it can be seen that the H_2SO_4 stratification in the AGM cell is much greater and the capacity drop is much deeper than for the MAGM cells. It can be assumed that the capacity fall at

Table 5
Average H_2SO_4 concentrations at Sep/PPlate and Sep/NPlate interfaces after cycling at 50 h discharge rate

Position	AGM		MAGM-L		MAGM-H	
	Immediately after discharge	After 24 h OC	Immediately after discharge	After 24 h OC	Immediately after discharge	After 24 h OC
Up	1.248	1.233	1.212	1.194	1.208	1.202
Middle	1.251	1.241	1.218	1.202	1.212	1.211
Bottom	1.276	1.265	1.240	1.246	1.240	1.232
Cell average concentration	1.258	1.246	1.223	1.214	1.220	1.215

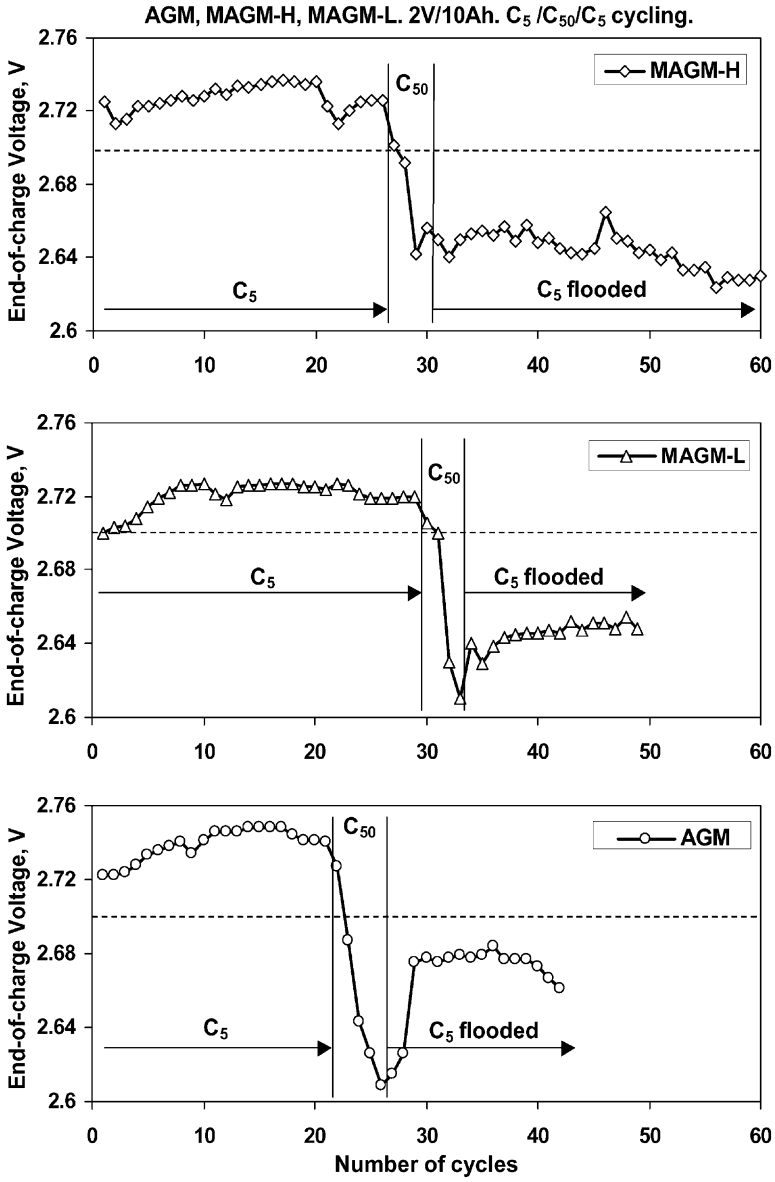

Fig. 13. End-of-discharge voltage vs. number of cycles curves for the three types of cells.

the beginning of cycling (Fig. 11) is caused by both vertical and horizontal stratification of H_2SO_4 in VRLA cells. As evident from the experimental results, *MAGM suppresses strongly the electrolyte stratification and increases the available capacity of the batteries on cycling*.

3.5. Influence of MAGM separator on the efficiency of the oxygen cycle and on water loss

The investigations were carried out with AGM and MAGM-H cells. The gas released from the cells was measured by the method described in [8]. The cells were cycled employing the following charge mode: $I_1 = 0.6C_5$ A up to $U = 14.8$ V. $U_2 = 14.8$ V up to 110% charge factor. Fig. 15 shows the amount of gas evolved by the cells with AGM and MAGM separators at every cycle.

It can be seen that the efficiency of the closed oxygen cycle is much higher in the cells with MAGM-H separators as compared to the AGM cells. Through measuring the cell weight it was found that the water loss on cycling of MAGM-H cells is four times smaller than that in AGM ones. In view of the reactions involved in the oxygen cycle (Fig. 5), it can be assumed that the MAGM-H separator facilitates the movement of O_2 and H^+ ions from the positive to the negative plates and of water in the opposite direction. Thus, the efficiency of the oxygen cycle is improved and the water loss is reduced.

Hence, MAGM-H is not only a continuous network of fibres with hydrophilic properties, but it contains a polymer component with hydrophobic properties. The latter is adsorbed onto the surface of the glass fibres, thus reducing the resistance in the passage of oxygen from the positive to the negative plates, which in turn improves the efficiency of

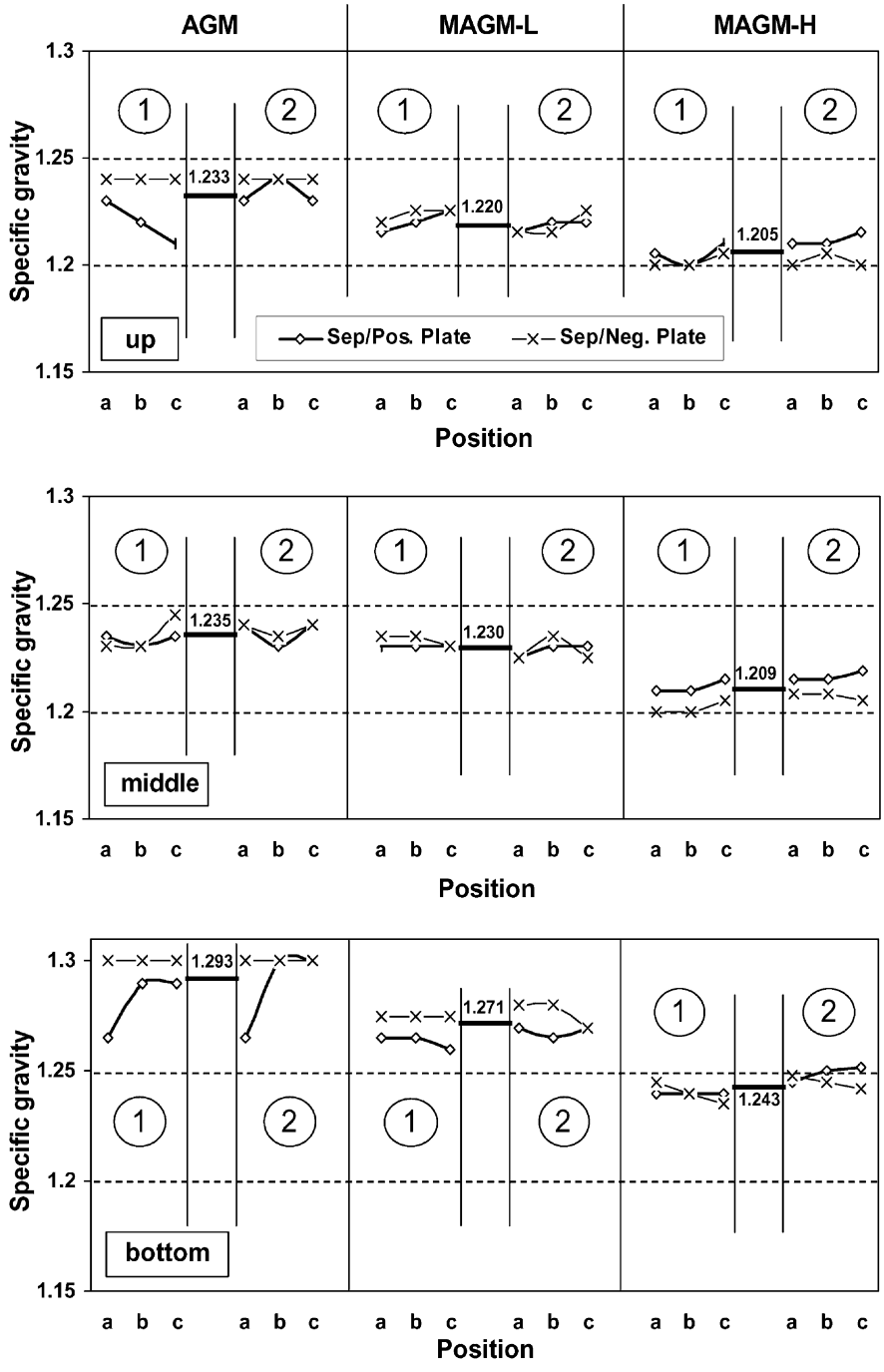

Fig. 14. H_2SO_4 concentrations at both interfaces of the two separators at the 20th cycle of the first stage of cycling measured (1) after discharge and (2) after 24 h rest on open circuit after 5 h discharge.

the oxygen cycle. The polymer component with hydrophilic properties is attached to the hydrophobic layer. The hydrophilic component of the polymer emulsion forms channels or layers along which water and H^+ ions move.

3.6. Influence of compression of the active block on H_2SO_4 concentration at the two separator interfaces on charging

The H_2SO_4 concentration was measured at the two separator interfaces (in the three horizontal zones) of charged plates at 8 and 25% active block compression. The concentrations at the two separator interfaces for the AGM and MAGM-H cells are given in Figs. 16 and 17, respectively.

The following conclusions can be drawn from the data in the figures:

AGM cell (Fig. 16): The H_2SO_4 concentration in the separator is influenced strongly by the compression. With increase of compression, the $C_{H_2SO_4}$ at the positive plate interface after charge increases in the upper and bottom

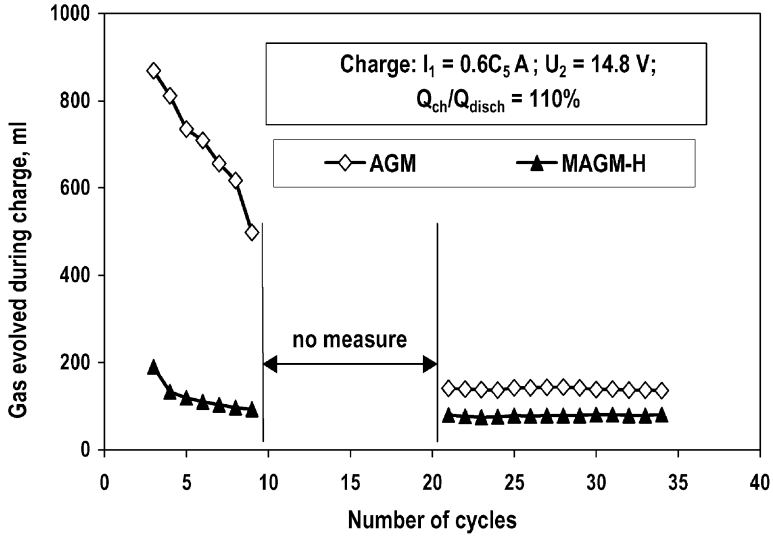

Fig. 15. Volume of gas released by the cells with AGM and MAGM-H separators on cycling.

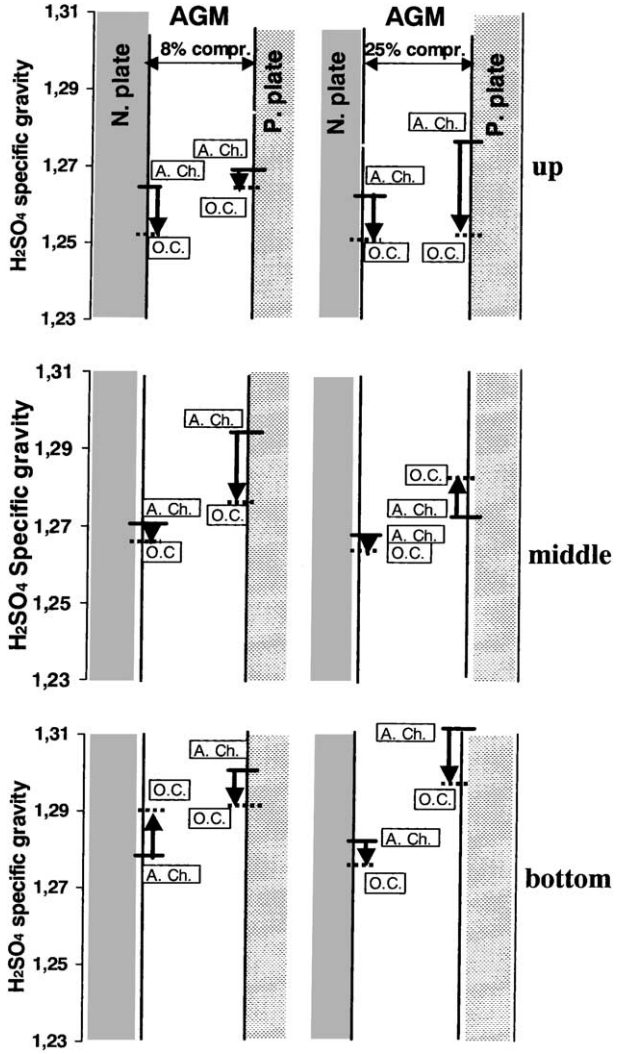

Fig. 16. H_2SO_4 concentration at the two separator interfaces for AGM cell after charge and at OC when either 8 or 25% compression was applied.

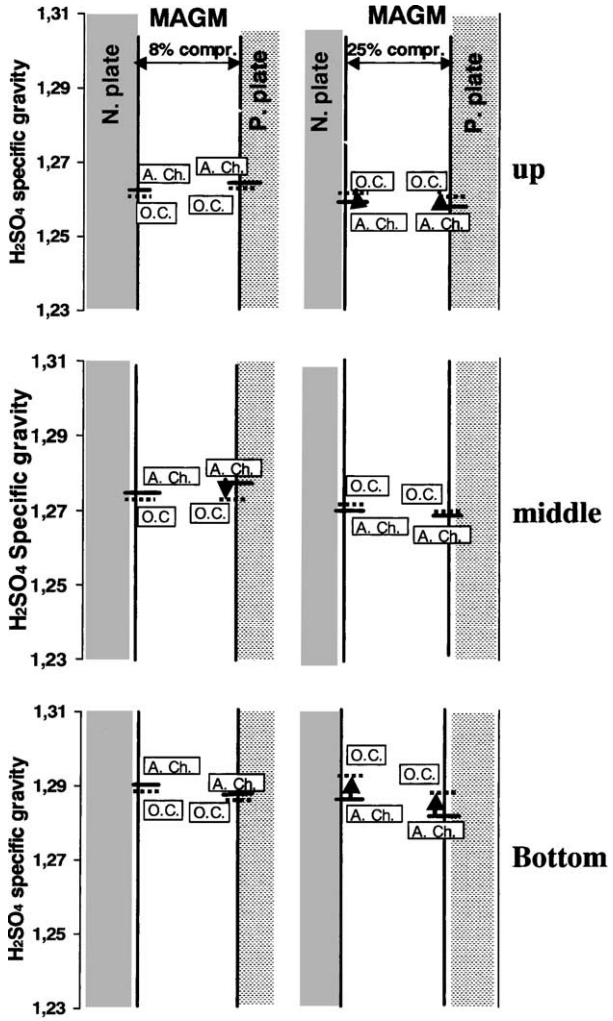

Fig. 17. H_2SO_4 concentration at the two separator interfaces for MAGM-H cell after charge and at OC when either 8 or 25% compression was applied.

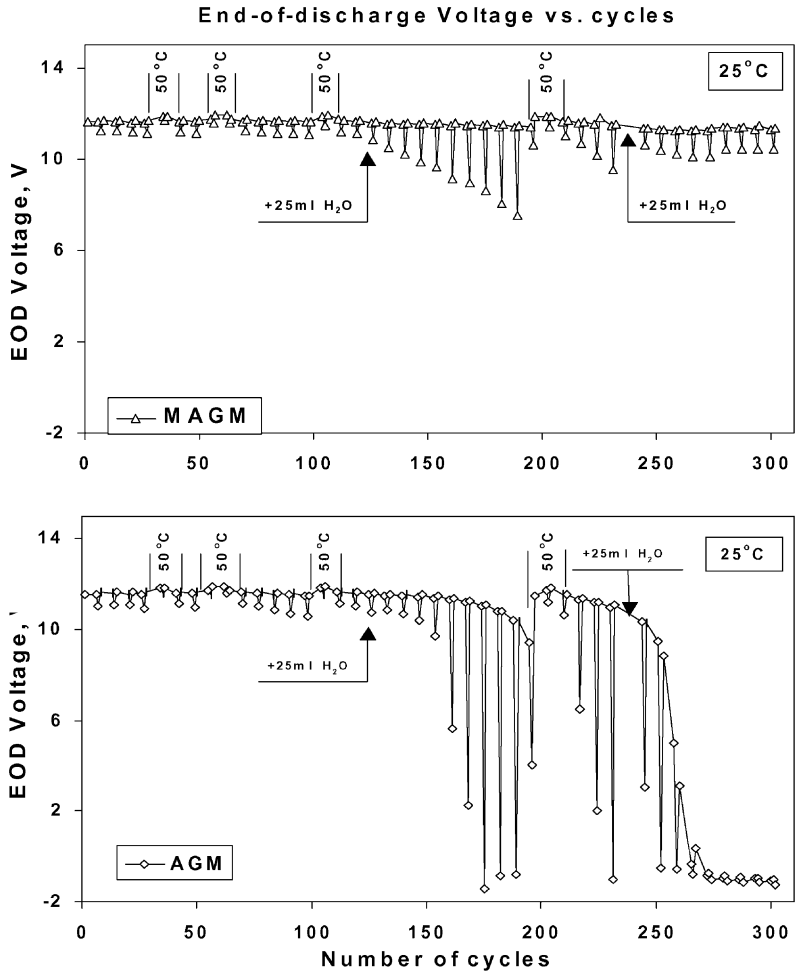

Fig. 18. End-of-discharge voltage (at 80 and 100% DOD) for 12 V/33 Ah batteries with AGM and MAGM separators cycled at 5 h rate of discharge.

zones of the cell, whereas in the middle zone it decreases. This shows a heterogeneous distribution of the rate of charge reactions in the positive plate. On hold of the cell on open circuit the H_2SO_4 concentration in the separator mostly decreases.

MAGM-H cell (Fig. 17): The concentration of H_2SO_4 in the separator decreases slightly or remains almost unchanged with increasing the compression of the active block. On open circuit rest, the H_2SO_4 concentration increases slightly in the middle and bottom zones of the compressed cell and it does not change in the remaining zones.

It can be generally concluded that increased compression of the active block has almost no effect on the MAGM-H cell but exerts a strong influence on the cells with AGM separator.

3.7. Influence of MAGM separator on battery performance: tests of traction and stand-by batteries

3.7.1. Cycle life tests of batteries with MAGM-H and AGM separators

Batteries (33 Ah) were assembled with three positive and four commercial negative plates per cell separated by AGM or MAGM-H separators (without the thin outer layers designed for measuring the $C_{H_2SO_4}$). We will use further the designation MAGM for the MAGM-H separator, which has proved to have the most beneficial effect on the performance of the lead-acid cell. The batteries were set to cycling tests at 5-h rate of discharge and 80% DOD. After every six cycles, a deep discharge (100% DOD)

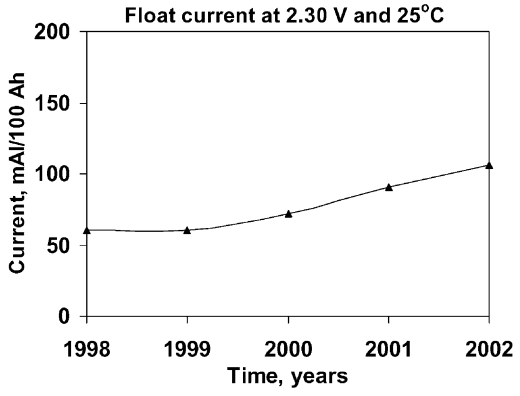

Fig. 19. Average float current at 2.30 V as a function of time of operation.

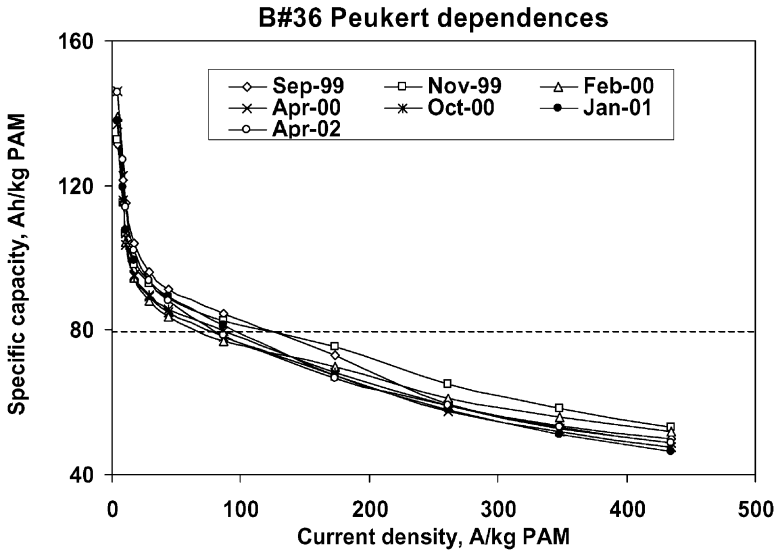

Fig. 20. Peukert dependencies for the batteries with MAGM separators determined after various periods of operation.

followed. The battery voltage was measured at the end of each discharge. The obtained results are presented in Fig. 18.

At certain time intervals the batteries were heated to 50 °C for 3 days. This treatment caused the capacity of both batteries to increase. However, as a result of the heating the batteries lost part of their water and had to be topped up with 25 ml H_2O per cell after the 125th and the 235th cycles.

The battery with AGM separator had a cycle life of about 150 cycles. After heating and watering, this battery endured another 50 cycles before failure.

The battery with MAGM separator exhibited a decline in available capacity after about 150 cycles, but after heating and watering the capacity increased and remained high for another 150 cycles. The test of this battery was interrupted after cycle 300 and it was subjected to post-mortem analysis. It was established that both the plates and the separators were in very good condition.

3.7.2. *Long-term tests of stand-by batteries with MAGM separators*

Tests were conducted with 12 V/40 Ah batteries with MAGM separators and PbSnCa grids. The tests included float charging at 2.30 V and 25 °C. Peukert dependence determinations were performed periodically and the changes in float current at 2.30 V were measured as a function of temperature.

Fig. 19 presents the dependence of the average float current on time. For 5 years, the float current has increased from 60 to about 100 mA/100 Ah at 2.30 V and 25 °C.

Fig. 20 shows the Peukert dependencies as determined seven times since September 1999. The capacity of the batteries as a function of current density has not changed much during this time.

The current at a charge voltage of 2.30 V as a function of the temperature is presented in Fig. 21. With increase of the temperature from 20 to 58 °C during float operation at 2.30 V, the current increases about eight times. The curve shows that this increase is more pronounced at temperatures above 38 °C.

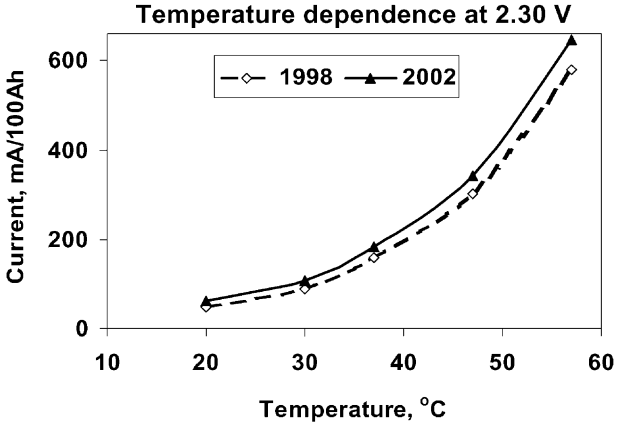

Fig. 21. Float current at charge voltage 2.30 V as a function of temperature.

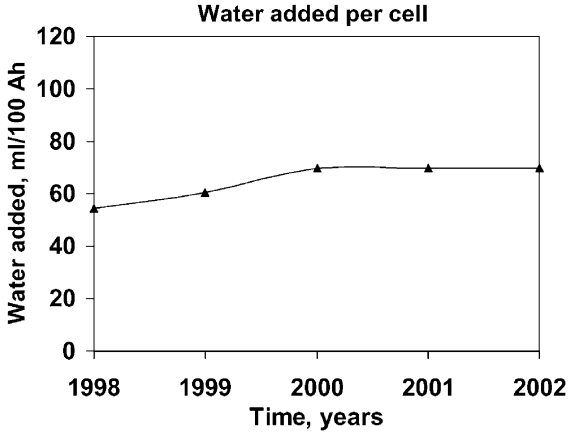

Fig. 22. Quantities of water added to the cells per year.

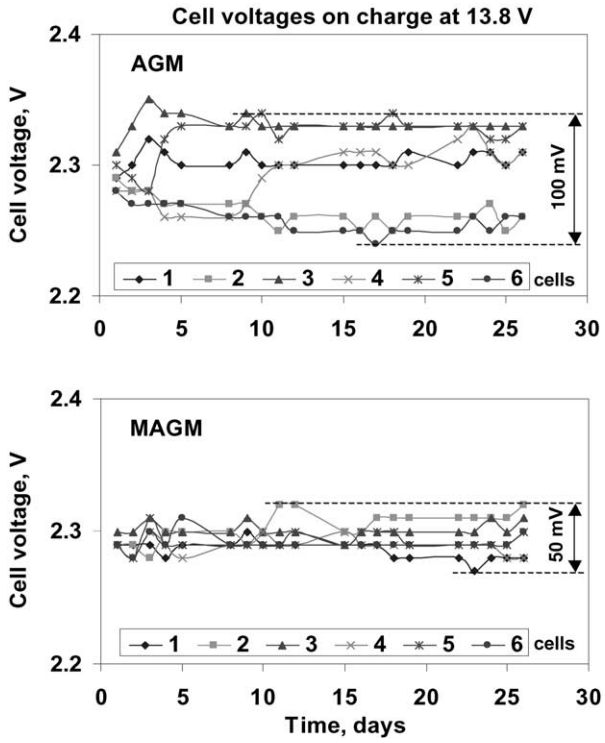

Fig. 23. Cell voltage for 12 V/40 Ah batteries with AGM and MAGM-H separators as a function of charging time at 13.8 V and 25 °C.

The potentials of the positive and of the negative half-cells were measured periodically, hence the cells were not sealed. Moreover, the batteries were heated to 50 °C several times for a period of 30 days. Consequently, water losses were observed, mainly through evaporation. This called for watering of the batteries once a year. Fig. 22 presents the quantities of water added to the cells by years. For 100 Ah cells the added water was about 70 ml per year. It can be expected that the water loss will be reduced substantially when the batteries are fitted with valves and the temperature of operation is 25 °C.

The results above discussed indicate that stand-by batteries with MAGM separators have fairly good performance characteristics when used in stand-by applications.

3.7.3. Influence of MAGM separators on the voltage deviation of cells connected into strings

As MAGM separators facilitate levelling of the H_2SO_4 concentration in the plates and in the separators, we measured the differences in cell voltage of the cells of two 12 V/40 Ah batteries, one with AGM and the other one with MAGM separators. The batteries were charged at 13.8 V and 25 °C for 1 month. Fig. 23 presents the measured cell voltages for the two batteries.

The difference in cell voltage for the battery with MAGM separators is half of that for the AGM battery. This indicates that MAGM separators are very suitable for use in cells interconnected in long strings, because they will reduce the voltage differences between the cells.

4. Conclusions

An experimental method has been devised for measuring the concentration of H_2SO_4 at the two separator interfaces: separator/positive plate and separator/negative plate. Using this method the difference between the H_2SO_4 concentrations at the two separator interfaces (i.e. the horizontal stratification) has been determined experimentally. This difference leads to the formation of acid concentration polarization, which results in a decline of VRLAB voltage and capacity.

By modifying the surface properties of the AGM separator through treatment with special polymer emulsions a new modified AGM separator has been created (MAGM). The latter facilitates the transport of H^+ ions, H_2O and H_2SO_4 between the positive and negative plates, and reduces the concentration polarization created in the cells during charge, discharge and on cycling.

The exchange of H_2SO_4 between the plates and the separator depends strongly on the charge or discharge rates and is limited by the surface properties of the separator fibres. These properties should differ for the two separator surfaces facing the positive and the negative plates, respectively. Hence, the MAGM separator should comprise two layers with different surface properties, which would reduce the electrolyte stratification and hence improve the performance of the battery.

Due to the above properties, the MAGM separator affects the performance of lead-acid batteries in their various applications. The use of MAGM separator improves substantially the cycle life of VRLA batteries and their available capacity on cycling. Moreover, the MAGM separator slightly lowers the end-of-charge voltage and shortens the charge duration. Stand-by batteries with MAGM separator have stable and very efficient performance parameters. MAGM separators decrease the voltage differences between the cells interconnected into networks. MAGM separators improve the efficiency of the oxygen cycle and reduce the water loss during battery operation.

Modification of AGM separators with polymer emulsion is simple from a technological point of view. The materials used are inexpensive commercial products of the chemical industry.

Acknowledgements

The authors thank GNB Technologies for the financial support provided for part of the present investigations.

References

[1] W.G. Sunu, B.W. Burrows, in: J. Tomson (Ed.), Power Sources, vol. 8, Academic Press, 1981, p. 601.
[2] F. Mattera, D.U. Sauer, D. Demesttre, M. Rosa, in: Proceedings of the LABAT'99, Abstract No. 48, Sofia, Bulgaria, p. 181.

[3] D.U. Sauer, J. Power Sources 64 (1997) 181.
[4] Bulgarian Patent 62 422.
[5] US Patent Application No. 09/423,026.
[6] D. Pavlov, I. Balkanov, P. Rachev, J. Electrochem. Soc. 134 (1987) 2390.
[7] D. Pavlov, E. Bashtavelova, V. Iliev, in: Proceedings of the 32nd Meeting of ISE, Part I, Dubrovnik, Yugoslavia, 1981, p. 146.
[8] D. Pavlov, S. Ruevski, V. Naidenov, G. Sheytanov, J. Power Sources 85 (2000) 164.